ALTRAS-CNFET: Full-Band Based Quantum Transport Simulator for Carbon Nanotube Field Effect Transistor Engineering: From Chirality to Device Performance

Yadong Tao [*], Feng Liu [**], Wei Bian [*], Tsz Yin Man [***], Mansun Chan [***] and Jin He [*,**,***]

[*] School of Computer & Information Engineering, Shenzhen Graduate School, Peking University, Shenzhen, 518055 P.R. China

[**] The Hub of Multi-Project-Wafer (MPW), Institute of Microelectronics, School of Electronic Engineering and Computer Science, Peking University, Beijing, 100871, P.R. China

[***] Department of Electronic and Computer Engineering, the Hong Kong University of Science & Technology, Clearwater Bay, Kowloon, 999077 HK jinhe@ime.pku.edu.cn

ABSTRACT

As one of the most promising alternative structures of silicon CMOS, Carbon Nanotube Field Effect Transistor (CNFET) has been paid lots of attention. The predicted dependences of band structure and device performance on chirality of Carbon Nanotube (CNT) and device structure have been studied in this paper by the means of a full-band based quantum transport simulator, ALTRAS-CNFET, developed by the group of Nano- & Tera- Devices and Circuits in Peking University. The results can be used to design and optimize the electrical characteristics of CNFET.

Keywords: Carbon Nanotube (CNT), Carbon Nanotube Field Effect Transistor (CNFET), band structure, quantum transport, direct tunneling gate current, sub-threshold swing

1 INTRODUCTION

Along with aggressive scaling of conventional silicon CMOS devices, on one hand, it seems that the scaling limit will be reached in one or one and half decade. On the other hand, new materials and technologies are being extensively studied as possible successors to silicon. At this crucial transition, Carbon Nanotube (CNT) may be one of the most promising structures because of a number of advantages such as ideal scalability, tunable band gap, strong covalent bonding, possible ballistic transport**,** High thermal conductivity and biological self-assembly [1].

To study CNT advanced performance and apply them to devices adequately, the band structure characteristics and the device configuration optimization are critical for CNT transistor application. In recent years, a lot of efforts have been devoted to CNT band structure modeling, and some important results have been obtained. For example, a detailed derivation of the energy dispersion relation is obatined by Saito et al based on a tight-binding approximation [2]. In the meantime, Carbon Nanotube Field Effect Transistor (CNFET) has been fabricated in various CNT configurations and their performances have been studied in details [3-6].

In this paper, a full-band based quantum transport simulator for CNFET engineering from chirality to device performance, ALTRAS-CNFET, is developed and further used to test CNFET performance. Including the modification of curvature effect, the band structure of CNT is obtained by the tight-binding approach. The self-consistent Schrödinger–Poisson equations were employed to calculate the direct tunneling gate current in the coaxial CNFET radial direction under cylindrical coordinates [7]. Based on the ballistic transport mechanism [8], the electrical characteristic in the coaxial CNFET channel direction is also computed. As a consequence, we have directly obtained CNFET electronic structure such as E-K relationship and electrical characteristics such as the dependence of the drain current and the direct tunneling gate current on gate voltage from this powerful simulator, which does not cost highly computational resources and time consumption.

2 SIMULATION PROCESS

2.1 Energy-band Structure of CNT

Following Anantram et al's method [2], the CNT is treated as a roll up graphite sheet and assumed a single pi orbit per carbon atom. The three vectors in tight-bind model, however, are not in the same plane due to curvature effect. Taking zigzag CNT (n, 0) as illustration, a sketch for denoting the change of vectors is shown in Fig.1.

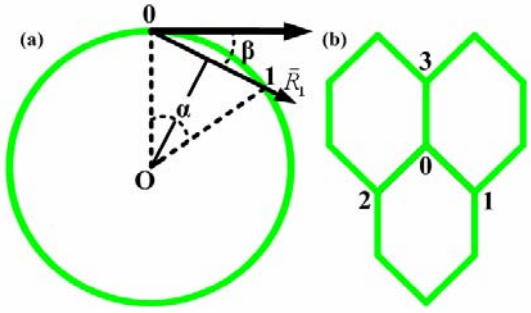

Fig.1 (a) the cross section along the line 0-1 parallel to the paper plane. (b) the corresponding graphite crystal lattice.

It is obvious that the C-C bonding is bended according to curvature effect, as shown in Fig.1 (a), arc (0, 1) being the C-C bonding distance. However, the magnitude of the vector $\vec{R}_1$ is no longer the C-C bonding distance but the

distance between 0 and 1. The changes on $\vec{R}_2$ and $\vec{R}_3$ are same as that of $\vec{R}_1$. The number of carbon atom in the cross section is n and the angle between O0 and O1 is tagged as α, which can be obtained as $\alpha = \frac{\sqrt{3}a_0}{r}$ where a_0 is the C-C bonding distance and r is the diameter of the CNT with $r = \frac{3na_0}{2\pi}$. The angle β is half of α, i.e. $\beta = \alpha/2$. As a result, considering the curvature effect, the three vectors can be modified as [9, 10]

$$\begin{cases} \vec{R}_1 = \frac{1}{2}a_0\vec{i} + r\sin\alpha\,\vec{j} - 2r\sin^2\frac{\alpha}{2}\vec{k} \\ \vec{R}_2 = \frac{1}{2}a_0\vec{i} - r\sin\alpha\,\vec{j} - 2r\sin^2\frac{\alpha}{2}\vec{k} \\ \vec{R}_3 = a_0\vec{i} \end{cases} \quad (1)$$

Putting the three vectors into the tight-binding approach with the periodic boundary condition around the circumference $n\sqrt{3}ka_0 = 2\pi q$, where k is the wave vector component along the circumference direction and q is an integer, the band structure of zigzag CNT (n, 0) containing the modification of curvature effect is written as

$$E(k) = \pm t\left[1 \pm 4\cos(q\sin\alpha)\cos\left(\frac{3}{2}a_0k + 2r\sin^2\frac{\alpha}{2}k\right) + 4\cos^2(q\sin\alpha)\right]^{1/2} \quad (2)$$

Employing the same method on the chiral CNT specified by (n, m), the Corresponding three vectors are as follows

$$\begin{cases} \vec{R}_1 = r\sin\alpha\,\vec{i} - 2r\sin^2\frac{\alpha}{2}\vec{k} \\ \vec{R}_2 = -r\sin\frac{\alpha}{2}\vec{i} + \frac{\sqrt{3}}{2}a_0\vec{j} - 2r\sin^2\frac{\alpha}{4}\vec{k} \\ \vec{R}_3 = -r\sin\frac{\alpha}{2}\vec{i} - \frac{\sqrt{3}}{2}a_0\vec{j} - 2r\sin^2\frac{\alpha}{4}\vec{k} \end{cases} \quad (3)$$

The amendatory energy band expression is obtained

$$E(k) = \pm t\left[1 + 4\cos(\frac{\sqrt{3}a_0k}{2})\cos\left(q\sin\frac{\alpha}{2} + q\sin\alpha\right) + 4\cos^2(\frac{\sqrt{3}a_0k}{2})\right]^{1/2} \quad (4)$$

The nanotube density of state is given by [11]

$$D_p(E) = \frac{8}{3\pi V_\Pi a_0}\frac{E}{\sqrt{E^2 - \Delta_p{}^2}} \quad (5)$$

Where, V_Π is the C-C bonding energy and Δ_p is the equilibrium conduction band minimum of the pth sub-band.

Using (3) or (4) and (5), the electron energy-band structure of CNT can be directly obtained in the ALTRAS-CNFET, and the results are employed in the following simulation steps.

2.2 Gate Tunneling Current in the Radial Direction of CNFET

The device geometry diagram of a coaxial CNFET with high-K is a long channel device as shown in Fig.2 for the simulation.

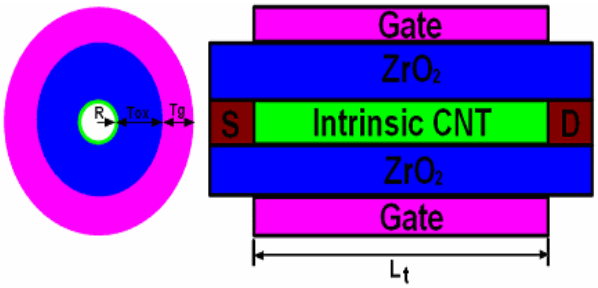

Fig.2 A physical diagram of a coaxial CNFET with length 100nm and high K dielectric.

Using the conventional central difference method and the resultant band gap and density of state, the simulator solves the Schrödinger and Poisson equations self-consistently in the radial direction under the cylindrical coordinates including the effect of wave function penetration into the gate electrode.

It is evident that the characteristic in every direction in the cross section is similar, so the one-dimensional form of Poisson equation under cylindrical coordinates is just focused in this study, the general form of which can be expressed as

$$\frac{\partial}{\partial r}\left(\varepsilon(r)\frac{\partial\Phi}{\partial r}\right) + \frac{\varepsilon(r)}{r}\frac{\partial\Phi}{\partial r} = -q\cdot Q(x) \quad (6)$$

Based on the same principle, the one-dimensional form of the time-independent effective mass Schrödinger equation under the cylindrical coordinates is written as

$$\frac{\partial}{\partial r}\left(\frac{1}{m^*(r)}\frac{\partial\Psi(r)}{\partial r}\right) + \frac{1}{m^*(r)}\frac{1}{r}\frac{\partial\Psi(r)}{\partial r} = \left(q\phi(r) - E\right)\Psi(r) \quad (7)$$

The carrier distribution is calculated by

$$n(r) = \sum 2m_dD_p(E)\sum\ln\left[1 + e^{(E_F - E)/kT}\right]\Psi(r)^2 \quad (8)$$

where the factor of two is due to the fact that Pauli exclusion principle allows two electrons per energy level: one spins up and another spins down, and m_d is the density-of-state effective mass.

The boundary condition implemented in the simulator is expressed as

$$\left.\frac{d\phi}{dr}\right|_{r=0} = 0 \quad \text{and} \quad \phi|_{r=R+T_{ox}} = \phi_s \quad (9)$$

Where, R is the radius of CNFET and T_{ox} is the oxide thickness. In the gate electrode, the wave function is treated as a traveling plane wave, which can be expressed into the following equation

$$\Psi_{-1} = \exp\left(ik\Delta x_{-1}\right)\Psi_0 \quad (10)$$

Where, Δx_{-1} is the uniform mesh spacing between the grid points. The probability current density can be obtained as

$$P_j = \frac{\hbar}{i2m_g}\left(\Psi^*_j\cdot\frac{\partial\Psi_j}{\partial x} - \frac{\partial\Psi^*_j}{\partial x}\cdot\Psi_j\right) \quad (11)$$

which is used to calculate the gate tunneling current density

$$J_G = -q\sum_j N_j^{inv}P_j \quad (12)$$

NSTI-Nanotech 2007, www.nsti.org, ISBN 1420061828 Vol. 1, 2007

By substituting equation (10) into (11), the gate tunneling current density (12) can be calculated quantum mechanically following [7]

$$J_G = q\sum_j N_j^{inv}\sqrt{2(E-E_g)/m_g}\,\Psi_{0,j}^2 \qquad (13)$$

Where, N_j^{inv} is the total inversion charge density in each energy level j, E_g and m_g are the conduction band edge and effective carrier mass in the gate electrode, respectively.

2.3 Electrical Characteristic in the Channel Direction of CNFET

Based on Anisur Rahman et al's model [8], it is assumed that the source Fermi level is the reference potential and immediately $\mu_S = 0$ and $\mu_D = -qV_{DS}$ are obtained. As a consequence, the total drain current I_D in the CNT channel direction can be analytical expressed as

$$I_{DS} = \frac{4qk_BT}{h}\sum\left[\ln\frac{1+e^{(E+U_t-E_F)/kT}}{1+e^{(E+U_t-qV_{DS}-E_F)/kT}}\right] \qquad (14)$$

Where, U_t is the electrostatic potential at the top of barrier.

Since it is known that there is a relation between the mobile charge and electrostatic potential, the quantum capacitance can be calculated by

$$C_Q = -q^2\frac{\partial(N_m)}{\partial(U_t)} \qquad (15)$$

From the perspective of the MOSFET device physics, the voltage gain and sub-threshold swing are also achieved accurately according to eq (16).

$$A_V = \frac{g_m}{g_d} = \frac{\partial I_D/\partial V_{GS}}{\partial I_D/\partial V_{DS}} \quad \text{and} \quad S \approx \frac{\partial V_{GS}}{\partial\log(I_{DS})} \qquad (16)$$

3 RESULTS AND DISCUSSION

In order to test the validity of the ALTRAS-CNFET simulator, two semiconducting CNTs specified by (7, 0) and (6, 2) were fed into this simulator. As a result, Comparing with the model without considering curvature effect, better band structure diagram is obtained shown in Fig.3. The density of state is calculated correctly in Fig.4.

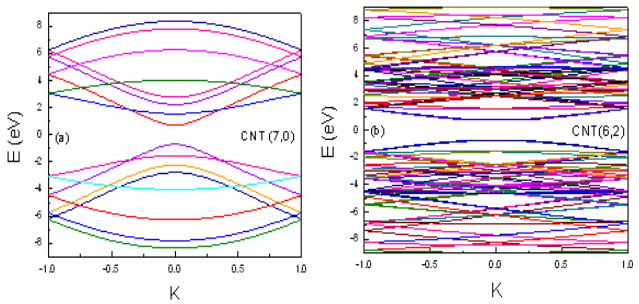

Fig.3 the band structure of two semiconducting CNTs specified by (a) (7, 0) and (b) (6, 2).

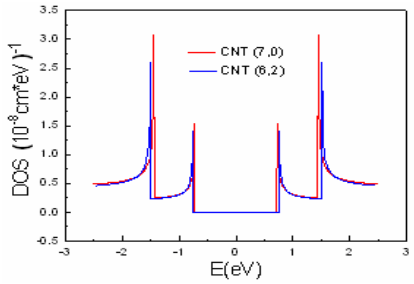

Fig.4 the dependence of density of state on energy for the two CNTs specified by (7, 0) and (6, 2).

The resultant electrostatic potential distribution in the radial direction is illustrated in Fig.5 when V_{GS} is 0.3V, 0.7V and 1V respectively. Simultaneously the carrier distribution in the radial direction is shown in Fig.6 when V_{GS} is 0.6V, 0.8V and 1V, respectively.

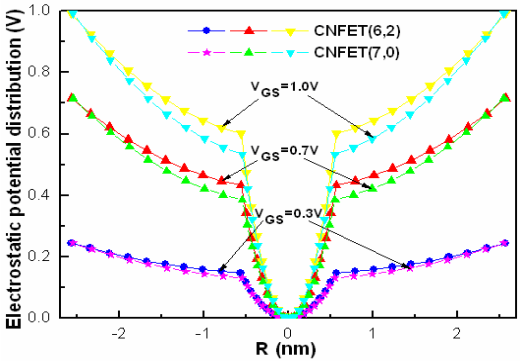

Fig.5 Plot of the electrostatic potential distribution in the radial direction when V_{GS} is 0.3V, 0.7V and 1V.

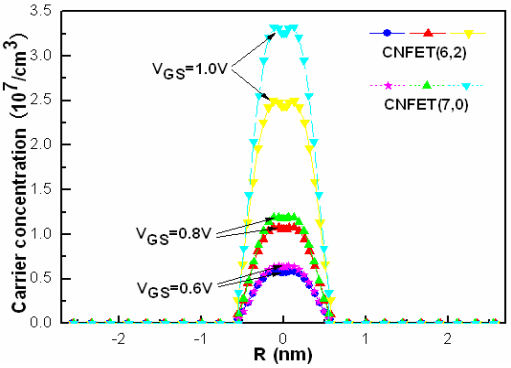

Fig.6 Plot of the carrier distribution in the radial direction when V_{GS} is 0.6V, 0.8V and 1V, respectively.

The dependence of direct tunneling gate current on the gate voltage for different oxide thickness is plotted in Fig.7.

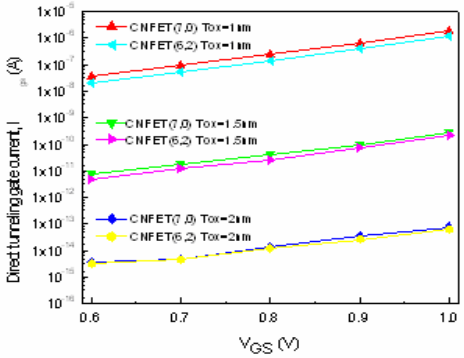

Fig.7 Plot of the direct tunneling gate current versus the gate voltage of the two coaxial CNFETs for three different oxide thicknesses: 1nm, 1.5nm and 2nm. V_{GS} is from 0.6V to 1.0V with a step size of 0.1V.

The pictures of I_{DS} versus V_{GS} and I_{DS} versus V_{DS} are shown in Fig.8 and Fig.9, respectively.

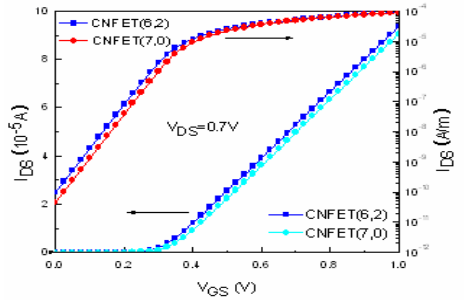

Fig.8 Plot of I_{DS} versus V_{GS} of the two coaxial CNFETs linearly and logarithmically when V_{DS} is 0.7V.

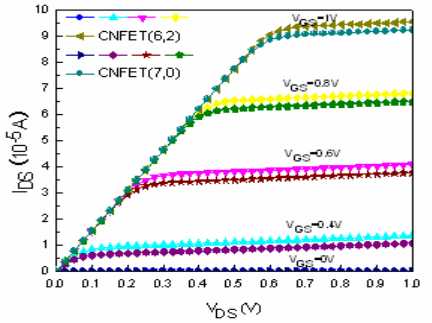

Fig.9 Plot of I_{DS} versus V_{DS} for different V_{GS} of the two CNFETs. V_{GS} is from 0V to 1V with a step size of 0.2V.

Figs.10 and 11 is the obtained Quantum capacitance, voltage gain versus V_{GS} and sub-threshold swing versus I_{DS}, respectively, from ALTRAS-CNFET.

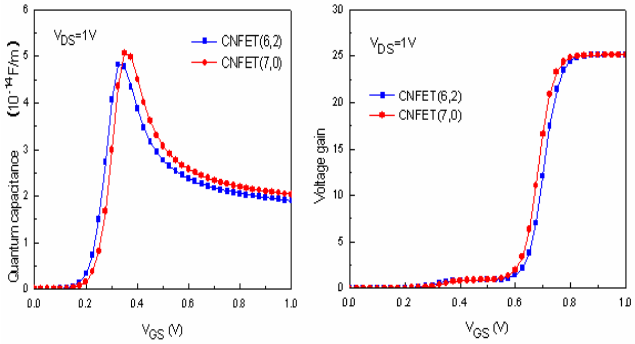

Fig.10 Plot of the quantum capacitance and voltage gain as a function of gate voltage of the two coaxial CNFETs when V_{DS} is 1V.

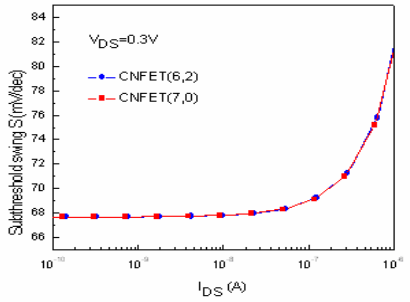

Fig.11 Plot of the extracted sub-threshold swing from the output characteristic as a function of I_{DS} for the two coaxial CNFETs when V_{DS} is 0.3V.

From the point of the device simulation, such a powerful simulator is easy-to-use and does not cost highly computational resources and time consumption. It is shown that that the drain current increases obviously with the oxide thickness dropping, which is ascribed to the increase of the induced charge due to the thinner oxide layer. The use of high K gate dielectrics leads to higher induced charge in the channel, which can remarkably lower the gate tunneling and the parasitic capacitance between the gate and the source (and drain). The low quantum capacitance and sub-threshold swing provide an opportunity to effectively perform the excellent properties of CNFET. As the gate bias increases and the energy band moves down, the sub-bands are populated one after the other. It is necessary to extend it into all the populated sub-bands in order to gain large ranges of gate bias, which will be the future work.

4 SUMMARY AND CONCLUSIONS

In summary, ALTRAS-CNFET is a powerful simulator for CNTFET energy-band calculation and CNFET performance prediction. It can directly compute the gate tunneling current in the radial direction, drain current in the channel and other electrical characteristics correctly based on device geometry and CNT material characteristics. The predicted results indicate that CNT is the most promising successor to silicon and the coaxial CNFET is likely to operate excellently.

REFERENCES

[1] P. Avouris, J. Appenzeller, R. Martel and S. J. wind, Proceedings of the IEEE, 91(11), 1772-1784, 2003.

[2] L. Yang, M. P. Anantram and J. P. Lu, Phys. Rev. B, 60, 29, 13874-13878, 1999.

[3] A. Raychowdhury, S. Mukhopadhyay and K. Roy, IEEE Trans. on Computer-Aided Design of Integrated Circuit and System, 23(10), 1411-1420, 2004.

[4] J. Knoch, S. Mantl and J. Appenzeller, Solid-state Electronics, 49(1), 73-76, 2005

[5] D. L. John, L. C. Castro, J. Clifford and D. L. Pulfrey, IEEE Trans. on Nanotechnology, 2(3), 175-180, 2003.

[6] J. Appenzeller, R. Martel, V. Derycke, M. Radosavljevic, S. Wind, D. Neumayer and Ph. Avouris, Microelectronic Engineering, 64(1-4), 391-397, 2002.

[7] H. Iwata, Appl. Phys. 40, 4496-4500, 2001.

[8] A. Rahman, J. Guo, S. Datta and M. S. lundstrom, Trans. Electron Dev. 50, 9, 1853-1864, 2003.

[9] R. Saito, G. Dresselhaus, and M. S. Dresselhaus, Carbon, 33, 7, 883-891, 1995

[10] Xiaofeng Wang, Doctor Dissertation, PKU, 2004.

[11] J.W. Mintmire and C. T. White, Phys. Rev. Lett. 81, 12, 2506-2509, 1998.